J. Water Environ. Nanotechnol., 2(1): 26-33 Winter 2017

ORIGINAL RESEARCH PAPER

Removal of nickel (II) from aqueous solution by graphene and boron nitride nanosheets

Jafar Azamat

Department of Chemical Engineering, Ahar Branch, Islamic Azad University, Ahar, Iran

Received: 2016.07.25 Accepted: 2016.09.18 Published: 2017.01.30

ABSTRACT

Molecular dynamics simulations were carried out to study the removal of Ni^{2+} as a heavy metal from the water by the functionalized graphene nanosheet (GNS) and boron nitride nanosheet (BNNS). Nickel causes asthma, conjunctivitis and inflammatory reactions and nickel salts act as emetics when swallowed; therefore, removal of nickel is necessary from the aqueous solutions. The systems were comprised of a nanosheet (GNS or BNNS) with a pore in its center that it is containing an aqueous ionic solution of nickel chloride. For the removal of Ni^{2+} from an aqueous solution, the pores of nanosheet were functionalized by passivating each atom at the pores edge and then an external electric field was applied along the z-axis of the simulated system. To justify the passage of ions through the pores, the potential of the mean force (PMF) of ions was calculated. To evaluate the properties of the system, the ion retention time and the radial distribution functions of species were measured. Based on the findings of this study, these nanostructure membranes can be recommended as a model for removal of heavy metals.

Keywords: Ni^{2+}; GNS; BNNS; PMF; Heavy metal.

How to cite this article

Azamat J. Removal of nickel (II) from aqueous solution by graphene and boron nitride nanosheets. J. Water Environ. Nanotechnol., 2017; 2(1): 26-33. DOI: 10.7508/jwent.2017.01.004

INTRODUCTION

Many toxic heavy metals are frequently discharged into the environment in the form of industrial wastewater, causing serious soil as well as water pollution. The wastewater discharged directly into natural water bodies is highly harmful to the aquatic ecosystems. Among these heavy metal species, Ni (II) has been frequently identified as a contaminant because of its high toxicity, mobility and enormous use in different industries, including electroplating and the manufacture of steel, pigments and storage batteries [1]. Although Ni (II) plays a pivotal role as a micronutrient in the synthesis of vitamin B12, its affluence over tolerance limits can cause cancer of the lungs, nose and bones as well as nausea, cyanosis, rapid respiration and etc. For these reasons, the necessity to removal of Ni (II) from industrial effluents has been emphasized before they are discharged [2-4]. The main source of nickel pollution in the water was derived from processes such as galvanization, smelting, mining, dyeing operations, batteries manufacturing and metal finishing. Trace amounts of nickel are beneficial to human organism as an activator of some enzyme systems, but if it is beyond the scope of normal levels, different types of diseases have been occurred. Evidently it is most important to remove these toxic metals from wastewater prior to their discharge into natural water bodies as they are non-biodegradable and persistent. Technologies, such as chemical reduction, ion-exchange, adsorption, reverse osmosis, electro dialysis and nanofiltration have been proposed for the removal of heavy metals [5-10]. However, most of these processes are relatively complicated or do not work efficiently to reduce metal concentrations below regulatory standards. Thus, the removal

* Corresponding Author Email: jafar.azamat@yahoo.com

of heavy metal ions in an effective way is of great importance from the viewpoints of both scientific research and engineering application.

Recently, membrane techniques have been introduced to remove heavy metal ions from water. Nanosheet membranes have been also used for the removal of various heavy metals [11], because they can separate ions and molecules. Ion separation using nanosheet membranes is done via pores created in them [12]. Graphene nanosheet (GNS) and boron nitride nanosheet (BNNS) are examples of nanostructured membranes. GNS is a carbon based nanomaterial with layers of carbon atoms densely packed in a honeycomb crystal lattice composed of two equivalent carbon sub-lattices [13]. GNS have some significant advantages in the preparation of carrier matrix due to their high surface area and remarkable mechanical stiffness and it exhibits a number of intriguing unique properties, such as high surface area of over 2600 m^2/g, large surface-to-volume ratio, high room temperature carrier mobility and conductance quantization. GNS has a wide range of possible membrane applications because of its ultimate thinness, flexibility, chemical stability and mechanical strength [14]. Recently, ion and gas separation through GNS by molecular dynamics (MD) simulation method have been studied [15-18]. The results of these works show that GNS with pores in its center can be efficiently utilized for separation technology.

For further investigation, BNNS was used also for the removal of nickel ions. A BNNS with a very high specific surface area exhibits excellent sorption performance for a wide range of oils, solvents, and dyes from water [19]. This membrane has unique properties, including a wide energy band gap, electrical insulation, ultraviolet photoluminescence, high thermal conductivity and stability, and high resistance to oxidation and chemical inertness [20-24]. This easy recyclability makes BNNS a good candidate for ion separation.

Perfect GNS and BNNS are impermeable to ions because there are no pores, and the electron density of their aromatic rings is enough to repel ions trying to pass through them. To pass ions through them, the drilling of pores is required. Functionalized pore in a nanosheet is obtained by passivating each atom at the pore edge using chemical functional groups. Herein, for nickel removal from an aqueous solution using a functionalized pore in center of GNS or BNNS, external electric field applied to the simulated system. We expect that our findings can be used to aid the design of nanostructured membranes for the removal of heavy metals for water treatment by nanostructure membranes such as GNS and BNNS.

SIMULATION METHOD

Fig. 1 displays an image of the simulation system. The size of the simulation box was $3\times3\times6$ nm^3. The box constituted of 1700 water molecules with 0.3 M $NiCl_2$ and a GNS or BNNS as a membrane was inside the box.

The full geometric optimization of a functionalized GNS and BNNS was calculated by the density functional theory method to obtain atomic charges and their optimized structures.

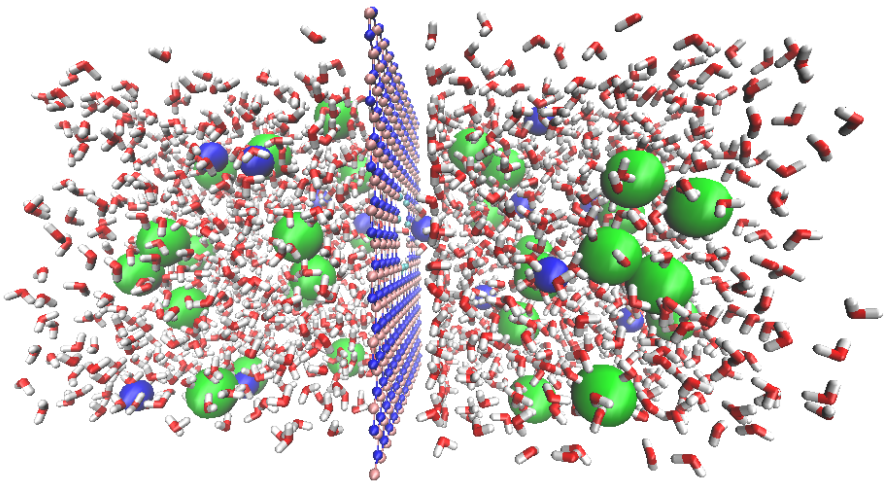

Fig. 1: A snapshot of the simulated system. The BNNS membrane with a functionalized pore in its center is located in the middle of simulation box (red: O, white: H, blue: Ni, and green: Cl).

These calculations were done using the GAMESS [25] at the B3LYP level of theory with 6-311G basis sets. The obtained results from DFT calculations for the functionalized membranes are given in Table 1.

As shown in Fig. 2, there were 377 carbon atoms and 9 fluorine atoms in the GNS and 183 nitrogen, 183 boron and 12 fluorine atoms in the BNNS. During the simulations, these membranes were held fixed. The diameter of the pores in the GNS and BNNS were about 0.6 nm and 0.8 nm, respectively.

Periodic boundary conditions were applied in the three directions. Water was modelled by using the simple point charge model [26]. Intermolecular interactions were described by the 12-6 Lennard-Jones (LJ) potential together with a Coulomb potential. The system was initially equilibrated at 298 K with a coupling time of 0.1 ps^{-1} for 1000 ps. In the modelling of sieving properties, our typical simulation runs were 5 ns long and obtained in the isobaric ensemble at the atmospheric pressure under applied electric field. The range of applied electric field was from 0 to 30 V, which is similar to other experimental studies in which the voltage is used to remove heavy metals [27]. The cutoff distance for nonbonding interactions was set up at 12 Å, and the particle mesh Ewald summations method was used to model the system's electrostatics [28]. During simulations, all the GNS and BNNS atoms were held in fixed positions. A time step of 1 fs was employed. At the beginning of each simulation run, water molecules rapidly filled the pore of membranes. Then after a certain period of time, ions started enter the pore. All MD simulations were carried out at constant

Table 1: Partial charges of GNS and BNNS atoms obtained from DFT calculations.

Atom	Charge (q)
Nitrogen	-0.4
Boron	0.4
Nitrogen bonded to Fluorine	0.25
Boron bonded to Fluorine	0.25
Fluorine of BNNS	-0.25
Carbon	0
Carbon bonded to Fluorine	0.29
Fluorine of GNS	-0.29

volume using the NAMD 2.10 [29] package with the CHARMM27 force field [30]. A Langevin thermostat and a hybrid Nose-Hoover Langevin piston were used to maintain the temperature and pressure of the system at 298 K and 1 bar, respectively. In this research, as in previous works [31-38], all analyses were performed using VMD 1.9.2 software [39]. The force field parameters for GNS and BNNS were obtained from [36,40] and nickel ions were modelled by using the parameters from reference [41].

The ion permeation from functionalized pores can be explained by calculating the potential of the mean force (PMF) [42]. The PMF was calculated by sampling the force experienced by ions that were placed at several positions along the z-axis of the box. In this work, each sampling window was run for 1 ns. The PMF of the ions was calculated using umbrella sampling [43] with either ion harmonically restrained in 0.1 Å steps in the axial z direction. Collective analysis was made using WHAM [44].

RESULTS AND DISCUSSION

To removal of Ni^{2+}, we used GNS and BNNS as a membrane with a functionalized pore in their

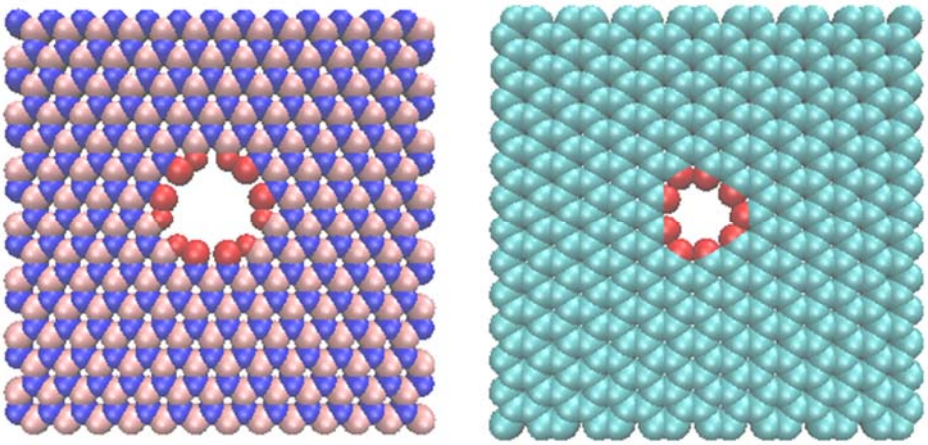

Fig. 2: Functionalized pore of membranes. Left: BNNS and right is GNS (blue represents nitrogen, silver is boron, cyan is carbon and red is fluoride).

centres under the influence of external voltage which was applied to the system, perpendicular to the pore of the membranes. With applying electric field, only nickel ions infuse through the functionalized pore of the membranes. Although GNS and BNNS have a large enough pore to accept nickel and chlorine ions, the results indicated that only Ni^{2+} permeates through these pores.

The MD results can be clarified by calculating the PMF of ions. We have done 50 ns MD simulation without applied electric field, to examine passage of ions in these conditions. It was observed that, any ions did not pass through the pores of GNS or BNNS. Therefore, we applied electric field for passage of ions from these pores. PMF can predict passing or rejecting of an ion across a path. Fig. 3 demonstrated the PMF for Ni^{2+} and Cl^- in the GNS and BNNS. As can be seen from Fig. 3, in both membranes, the energy barrier for chloride is higher than nickel. Thus, the chloride ion will not be able to cross the membrane. This is due to termination of functionalized pores of membranes by the negatively-charged atoms (fluoride atom), which favours the passage of cations.

Also, the PMF for Ni^{2+} in the BNNS is lower than the GNS. This trend leads to more Ni^{2+} permeating from the pore of the BNNS, in effect of identical applied electric field to GNS and BNNS. The Ni^{2+} permeated from functionalized pores when 5 and 7.5 V electric fields were applied to the BNNS and GNS, respectively. Fig. 4 shows the number of Ni^{2+} passing through the functionalized pore of the GNS and BNNS. With the increment of the applied electric field, the number of Ni^{2+} passing was increased. As seen in Fig. 4, Ni^{2+} passes through the pore of the BNNS more than the GNS. This is

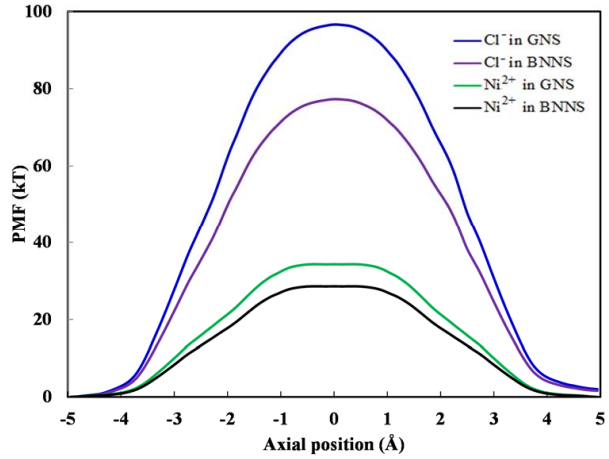

Fig. 3: The PMF for Ni^{2+} and Cl^- ions in the GNS and BNNS systems.

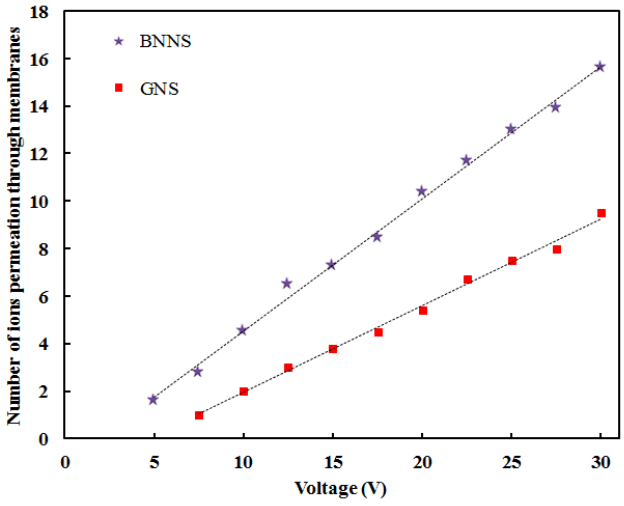

Figure 4. The number of Ni^{2+} passing through the pore of GNS and BNNS.

due to the low energy barrier of Ni^{2+} in the BNNS compared to that in the GNS.

The time required for a nickel ion to pass through the pore (retention time) is an important parameter. Fig. 5 shows the retention time of a Ni^{2+} ion as a function of applied electric field. Increasing the electric field has decreased the retention time.

Therefore, removal of heavy metal from the aqueous solution at high voltages happens quickly. The energy barrier in the PMF for Ni^{2+} in the pore of GNS is high compared to that of the BNNS pore. Thus, the retention time of the Ni^{2+} in the GNS system is greater than that of the BNNS. In the other words, nickel ions passes quickly through the BNNS pore.

To characterize the structure of water molecules around the ions, the radial distribution function (RDF) between the ion and water molecule was considered that it was obtained from the trajectory files of MD simulation. There is a clear maximum and minimum for each first RDF. These have been shown that a coordination shell of water exists around of ions. Fig. 6 shows the RDF Ni^{2+}-water in the GNS and BNNS systems. The first peak corresponds to the distribution of the neighbour water molecules around the nickel ions. For the RDF peaks of Ni^{2+} in the GNS and BNNS systems, the position and magnitude of the first maximum and minimum are almost identical. This indicates that the hydration number of this ion in both systems is identical.

On the other hand, the structure of water molecules around the membranes in both systems is similar. The water molecules have been shown a tendency to accumulate in the region at a location about ±4.5 Å from the GNS and BNNS. This structure is shown by two visible peaks in the density profile on each side (see Fig. 7).

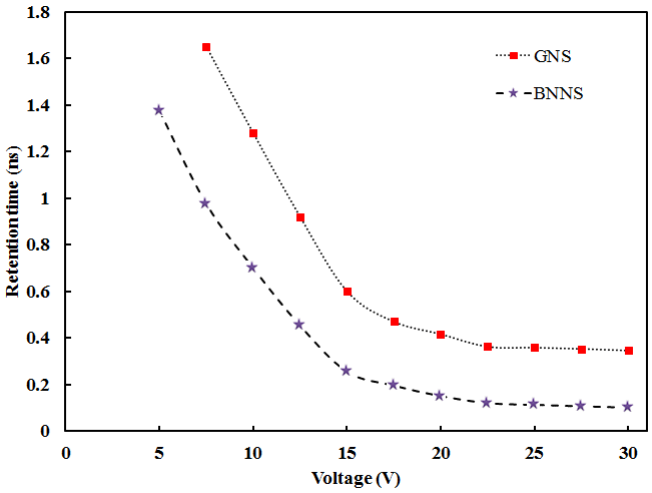

Fig. 5: Retention time for Ni^{2+} in various voltages in the GNS and BNNS.

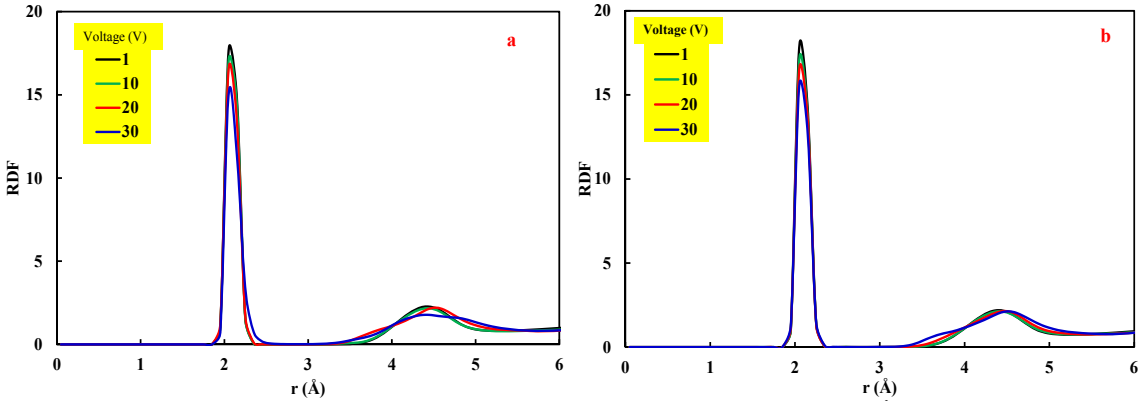

Fig. 6: RDFs under various voltages: (a) RDF Ni^{2+}- water in the GNS system, (b) RDF Ni^{2+}- water in the BNNS system.

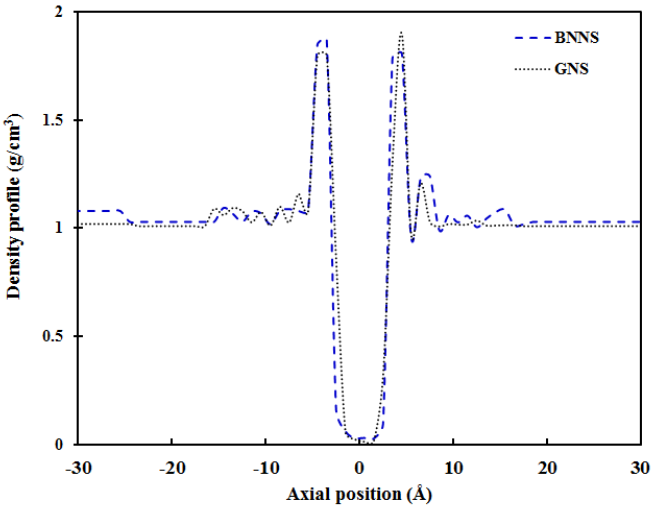

Fig. 7: Density profile of water molecules in the GNS and BNNS systems.

However, the number of Ni^{2+} passing through the GNS and BNNS is different. This indicates that structure of the water molecules were ineffective in the number of ions passing through the pores. Therefore, difference in the number of ions passing through the pores is related to the pore structure. This case is illustrated by the PMF, in which the barrier energy of Ni^{2+} ions in the BNNS is less than that of GNS. Thus, the retention time of the Ni^{2+} in the BNNS system is less than of the GNS system. Therefore, Ni^{2+} passes quickly through the pore of the BNNS.

When water molecules pass across the functionalized pores of GNS and BNNS, they form a single file structure. As can be seen in Fig. 7, the structure of water molecules on both sides of the membranes was different from water molecules in the bulk region. The density profile was calculated from histograms of the number of water molecules. The water molecules displayed a tendency to accumulate in the region at a location about ±4.5 Å from the GNS and BNNS. In fact, the density of water on both sides of the membranes was higher than that in the bulk water. This phenomenon occurred for both types of membranes. In the region far away from the membranes, the density of water was about 1 g/cm^3. The layered structure of water molecules in this region is due to the non-bonded interaction of membranes atoms, and water molecules.

CONCLUSION

MD simulations technique was used to investigate the removal of nickel ions as a heavy metal across functionalized pores of GNS and BNNS. Based on the results of PMF calculations, the GNS and BNNS were able to remove Ni^{2+} from aqueous solutions under applied electric field. Compared to the GNS, a BNNS can remove the Ni^{2+} from water efficiently. With increasing applied electric field to the considered systems, more ions could pass through the pore of membranes. In addition, with increasing applied voltage, the retention time of the ions decreased.

ACKNOWLEDGMENTS

Author thanks the Iranian Nanotechnology Initiative Council for the support provided.

CONFLICT OF INTEREST

The author declares that there are no conflicts of interest regarding the publication of this manuscript.

REFERENCES

1. Panneerselvam P., Morad N., Tan K. A., 2011. Magnetic nanoparticle (Fe_3O_4) impregnated onto tea waste for the removal of nickel (II) from aqueous solution. *J. Hazard. Mater.* 186: 160-168.
2. Babel S., Kurniawan T. A., 2003. Low-cost adsorbents for heavy metals uptake from contaminated water: a review. *J. Hazard. Mater.* 97: 219-243.
3. Wong S., Li X., Zhang G., Qi S., Min Y., 2002. Heavy metals in agricultural soils of the Pearl River Delta, South China. *Environ. Pollut.* 119: 33-44.
4. Nandi D., Saha I., Ray S. S., Maity A., 2015. Development of a reduced-graphene-oxide based superparamagnetic nanocomposite for the removal of nickel (II) from an

aqueous medium via a fluorescence sensor platform. *J. Colloid Interface Sci.* 454: 69-79.

5. Hegazi H. A., 2013. Removal of heavy metals from wastewater using agricultural and industrial wastes as adsorbents. *HBRC Journal* 9: 276-282.
6. Štandeker S., Veronovski A., Novak Z., Knez Ž., 2011. Silica aerogels modified with mercapto functional groups used for Cu(II) and Hg(II) removal from aqueous solutions. *Desalination* 269: 223-230.
7. Meena A. K., Mishra G. K., Rai P. K., Rajagopal C., Nagar P. N., 2005. Removal of heavy metal ions from aqueous solutions using carbon aerogel as an adsorbent. *J. Hazard. Mater.* 122: 161-170.
8. Chen G., 2004. Electrochemical technologies in wastewater treatment. *Sep. Purif. Technol.* 38: 11-41.
9. Borhade A. V., Kshirsagar T. A., Dholi A. G., Agashe J. A., 2015. Removal of heavy metals Cd^{2+}, Pb^{2+}, and Ni^{2+} from aqueous solutions using synthesized azide cancrinite, $Na_8[AlSiO_4]_6(N_3)_{2.4}(H_2O)_{4.6}$. *J. Chem. Eng. Data* 60: 586-593.
10. Zhang S., Cheng F., Tao Z., Gao F., Chen J., 2006. Removal of nickel ions from wastewater by $Mg(OH)_2$/MgO nanostructures embedded in Al_2O_3 membranes. *J. Alloys Compd.* 426: 281-285.
11. Goh P. S., Ismail A. F., 2015. Graphene-based nanomaterial: The state-of-the-art material for cutting edge desalination technology. *Desalination* 356: 115-128.
12. Suk M. E., Aluru N. R., 2010. Water transport through ultrathin graphene. *J. Phys. Chem. Lett.* 1: 1590-1594.
13. He Z., Zhou J., Lu X., Corry B., 2013. Bioinspired graphene nanopores with voltage-tunable ion selectivity for Na^+ and K^+. *ACS Nano* 7: 10148-10157.
14. Taherian F., Marcon V., van der Vegt N. F. A., Leroy F., 2013. What is the contact angle of water on graphene? *Langmuir* 29: 1457-1465.
15. Konatham D., Yu J., Ho T. A., Striolo A., 2013. Simulation insights for graphene-based water desalination membranes. *Langmuir* 29: 11884-11897.
16. Cohen-Tanugi D., Grossman J. C., 2012. Water desalination across nanoporous graphene. *Nano Lett.* 12: 3602-3608.
17. Drahushuk L. W., Strano M. S., 2012. Mechanisms of gas permeation through single layer graphene membranes. *Langmuir* 28: 16671-16678.
18. Sun C., Boutilier M. S. H., Au H., Poesio P., Bai B., Karnik R., Hadjiconstantinou N. G., 2013. Mechanisms of molecular permeation through nanoporous graphene membranes. *Langmuir* 30: 675-682.
19. Lei W., Portehault D., Liu D., Qin S., Chen Y., 2013. Porous boron nitride nanosheets for effective water cleaning. *Nat. Commun.* 4: 1777.
20. Golberg D., Bando Y., Huang Y., Terao T., Mitome M., Tang C., Zhi C., 2010. Boron nitride nanotubes and nanosheets. *ACS Nano* 4: 2979-2993.
21. Mortazavi B., Rémond Y., 2012. Investigation of tensile response and thermal conductivity of boron-nitride nanosheets using molecular dynamics simulations. *Physica E* 44: 1846-1852.
22. Lei W., Zhang H., Wu Y., Zhang B., Liu D., Qin S., Liu Z., Liu L., Ma Y., Chen Y., 2014. Oxygen-doped boron nitride nanosheets with excellent performance in hydrogen storage. *Nano Energy* 6: 219-224.
23. Sun Q., Li Z., Searles D. J., Chen Y., Lu G., Du A., 2013. Charge-controlled switchable CO_2 capture on boron nitride nanomaterials. *J. Am. Chem. Soc.* 135: 8246-8253.
24. Pakdel A., Zhi C., Bando Y., Golberg D., 2012. Low-dimensional boron nitride nanomaterials. *Mater. Today* 15: 256-265.
25. Schmidt M. W., Baldridge K. K., Boatz J. A., Elbert S. T., Gordon M. S., Jensen J. H., Koseki S., Matsunaga N., Nguyen K. A., Su S., Windus T. L., Dupuis M., Montgomery J. A., 1993. General atomic and molecular electronic structure system. *J. Comput. Chem.* 14: 1347-1363.
26. Berendsen H. J. C., Grigera J. R., Straatsma T. P., 1987. The missing term in effective pair potentials. *J. Phys. Chem.* 91: 6269-6271.
27. Bazrafshan E., Mahvi A. H., Zazouli M. A., 2011. Removal of zinc and copper from aqueous Solutions by electrocoagulation technology using iron electrodes. *Asian J. Chem.* 23: 5506-5510.
28. Essmann U., Perera L., Berkowitz M. L., Darden T., Lee H., Pedersen L. G., 1995. A smooth particle mesh Ewald method. *J. Chem. Phys.* 103: 8577-8593.
29. Phillips J. C., Braun R., Wang W., Gumbart J., Tajkhorshid E., Villa E., Chipot C., Skeel R. D., Kale L., Schulten K., 2005. Scalable molecular dynamics with NAMD. *J. Comput. Chem.* 26: 1781-1802.
30. MacKerell A. D., Bashford D., Bellott, Dunbrack R. L., Evanseck J. D., Field M. J., Fischer S., Gao J., Guo H., Ha S., Joseph-McCarthy D., Kuchnir L., Kuczera K., Lau F. T. K., Mattos C., Michnick S., Ngo T., Nguyen D. T., Prodhom B., Reiher W. E., Roux B., Schlenkrich M., Smith J. C., Stote R., Straub J., Watanabe M., Wiórkiewicz-Kuczera J., Yin D., Karplus M., 1998. All-atom empirical potential for molecular modeling and dynamics studies of proteins. *J. Phys. Chem. B* 102: 3586-3616.
31. Azamat J., Khataee A., Joo S. W., 2015. Molecular dynamics simulation of trihalomethanes separation from water by functionalized nanoporous graphene under induced pressure. *Chem. Eng. Sci.* 127: 285-292.
32. Azamat J., Khataee A., Joo S. W., 2015. Removal of heavy metals from water through armchair carbon and boron nitride nanotubes: a computer simulation study. *RSC Adv.* 5: 25097-25104.
33. Azamat J., Khataee A., Joo S. W., Yin B., 2015. Removal of trihalomethanes from aqueous solution through armchair carbon nanotubes: A molecular dynamics study. *J. Mol. Graphics Modell.* 57: 70-75.
34. Khataee A., Azamat J., Bayat G., 2016. Separation of nitrate ion from water using silicon carbide nanotubes as a membrane: Insights from molecular dynamics simulation. *Comput. Mater. Sci* 119: 74-81.
35. Azamat J., Sardroodi J. J., Mansouri K., Poursoltani L., 2016. Molecular dynamics simulation of transport of water/DMSO and water/acetone mixtures through boron nitride nanotube. *Fluid Phase Equilib.* 425: 230-236.

36. Azamat J., Khataee A., Joo S. W., 2016. Molecular dynamics simulations of trihalomethanes removal from water using boron nitride nanosheets. *J. Mol. Model.* 22: 1-8.
37. Azamat J., Balaei A., Gerami M., 2016. A theoretical study of nanostructure membranes for separating Li+ and Mg2+ from Cl–. *Comput. Mater. Sci* 113: 66-74.
38. Azamat J., Khataee A., Joo S. W., 2016. Separation of copper and mercury as heavy metals from aqueous solution using functionalized boron nitride nanosheets: A theoretical study. *J. Mol. Struct.* 1108: 144-149.
39. Humphrey W., Dalke A., Schulten K., 1996. VMD: Visual molecular dynamics. *J. Mol. Graphics* 14: 33-38.
40. Sint K., Wang B., Král P., 2008. Selective ion passage through functionalized graphene nanopores. *J. Am. Chem. Soc.* 130: 16448-16449.
41. Li P., Roberts B. P., Chakravorty D. K., Merz K. M., 2013. Rational design of particle mesh ewald compatible lennard-jones parameters for +2 metal cations in explicit solvent. *J. Chem. Theory Comput.* 9: 2733-2748.
42. Kjellander R., Greberg H., 1998. Mechanisms behind concentration profiles illustrated by charge and concentration distributions around ions in double layers. *J. Electroanal. Chem.* 450: 233-251.
43. Torrie G. M., Valleau J. P., 1977. Nonphysical sampling distributions in monte carlo free-energy estimation: Umbrella sampling. *J. Comput. Phys.* 23: 187-199.
44. Kumar S., Payne P. W., Vásquez M., 1996. Method for free-energy calculations using iterative techniques. *J. Comput. Chem.* 17: 1269-1275.